THE JOURNAL OF BIOLOGICAL CHEMISTRY VOL. 286, NO. 29, pp. 25655–25662, July 22, 2011

Mitochondrial Carnitine Palmitoyltransferase 1a (CPT1a) Is Part of an Outer Membrane Fatty Acid Transfer Complex*[S]

Received for publication, February 15, 2011, and in revised form, May 20, 2011 Published, JBC Papers in Press, May 26, 2011, DOI 10.1074/jbc.M111.228692

Kwangwon Lee[‡§], **Janos Kerner**[‡§], **and Charles L. Hoppel**[‡§¶1]

From the [‡]*Center for Mitochondrial Diseases and Departments of* [§]*Pharmacology and* [¶]*Medicine, Case Western Reserve University, Cleveland, Ohio 44106-4981*

CPT1a (carnitine palmitoyltransferase 1a) in the liver mitochondrial outer membrane (MOM) catalyzes the primary regulated step in overall mitochondrial fatty acid oxidation. It has been suggested that the fundamental unit of CPT1a exists as a trimer, which, under native conditions, could form a dimer of the trimers, creating a hexamer channel for acylcarnitine translocation. To examine the state of CPT1a in the MOM, we employed a combined approach of sizing by mass and isolation using an immunological method. Blue native electrophoresis followed by detection with immunoblotting and mass spectrometry identified large molecular mass complexes that contained not only CPT1a but also long chain acyl-CoA synthetase (ACSL) and the voltage-dependent anion channel (VDAC). Immunoprecipitation with antisera against the proteins revealed a strong interaction between the three proteins. Immobilized CPT1a-specific antibodies immunocaptured not only CPT1a but also ACSL and VDAC, further strengthening findings with blue native electrophoresis and immunoprecipitation. This study shows strong protein-protein interaction between CPT1a, ACSL, and VDAC. We propose that this complex transfers activated fatty acids through the MOM.

Long chain fatty acids, an important energy source in mitochondria, are oxidized in the matrix via β-oxidation. Long chain fatty acids are activated on the cytosolic side of the mitochondrial outer membrane (MOM)[2] by long chain acyl-CoA synthetase (ACSL) (1). To be metabolized, activated fatty acids, as well as other substrates, ions, and nucleotides, cross the MOM through the voltage-dependent anion channel (VDAC), also called mitochondrial porin.

Historically, the MOM was considered to be a sieve through which small compounds passed unimpeded. That view is no longer tenable. In *Trypanosoma brucei*, which expresses only one VDAC, knock-out of VDAC leads to mitochondria that no longer oxidize substrates (2). However, with disruption of the outer membrane, the mitoplasts are fully capable of oxidizing substrates. These studies highlight the essential role of VDAC in mitochondrial substrate oxidation in transportation of small anion substrates through the MOM.

We studied PA22, a 22-kDa polyanion VDAC inhibitor (3), in mitochondrial substrate oxidation and observed that ADP-stimulated glutamate, succinate, (+rotenone), and palmitoylcarnitine (+malate) oxidation rates were unaffected. However, oxidation of palmitate (+ATP, Mg^{2+}, CoA, carnitine, and malate) and palmitoyl-CoA (+carnitine and malate) was inhibited at 1–2 nmol of PA22/mg of mitochondrial protein. These data indicate that PA22 is selective for the first two steps in fatty acid oxidation without affecting other substrates. Additionally, we showed that PA22 interacts with VDAC by demonstrating that binding of hexokinase to rat liver mitochondria was inhibited by PA22 (3). VDAC was initially identified as the hexokinase-binding protein (4).

PA10, a 10-kDa polyanion VDAC inhibitor (5), decreases ADP-stimulated oxidation of glutamate, malate, and succinate. The inhibition of glutamate oxidation is relieved by high ADP or an uncoupler. In our studies, we showed that PA10 inhibited palmitoyl-CoA (+carnitine and malate) oxidation but that this inhibition was not relieved by high ADP. PA10 binds to VDAC as shown in electrophysiological experiments (6). In 1999, the reason for the specificity of the two polyanions was not apparent. However, we are now aware of three VDAC isoforms and that knock-outs of these produce different phenotypes (7). Mitochondria from VDAC1 knock-out mice, in particular, have a defect in ADP-stimulated oxidation (8), which is relieved by an uncoupler, whereas mitochondria from VDAC3 knock-out mice do not have any oxidative defects (9). VDAC also exists at the same time in different substates (10). These data indicate that VDAC1 transports ADP, although this is not the case for VDAC3 and is consistent with differing substrate specificity for VDACs.

The carnitine-dependent transport of activated fatty acids is catalyzed by CPT1a (carnitine palmitoyltransferase 1a), an integral outer membrane protein that converts activated fatty acids into acylcarnitines (11). Using size exclusion chromatography and blue native electrophoresis (BNE) of extracts of mitochondria isolated from livers of fed rats or *Saccharomyces cerevisiae* expressing CPT1a, Faye *et al.* (12) reported that CPT1a exists as a trimer, which, under native conditions, dimerizes to form hexamers. The authors proposed that trimeric CPT1a is arranged to form channels allowing acylcarnitines to enter the intermembrane space. Additionally, Jenei *et al.* (13) suggested that the interaction between the G*XXX*G and G*XXX*A motifs within transmembrane domain 2 of CPT1a leads to the hexamerization and stabilization of recombinant CPT1a. However,

* This work was supported, in whole or in part, by National Institutes of Health Grant DK-066107.

[S] The on-line version of this article (available at http://www.jbc.org) contains supplemental Fig. S1 and Tables S1–S3.

[1] To whom correspondence should be addressed: Case Western Reserve University, 10900 Euclid Ave., Cleveland, OH 44106-4981. Tel.: 216-368-3147; Fax: 216-368-5162; E-mail: charles.hoppel@case.edu.

[2] The abbreviations used are: MOM, mitochondrial outer membrane; ACSL, long chain acyl-CoA synthetase; VDAC, voltage-dependent anion channel; BNE, blue native electrophoresis.

the conclusion that CPT1a exists as a homo-oligomer is based solely on the finding that the observed higher molecular mass species of CPT1a could be accounted for by multiples of the monomeric mass of CPT1a. The important question is whether the hexameric CPT1a channel acylcarnitines or CPT1a forms hetero-oligomeric complexes with other metabolically relevant enzymes and channel proteins such as ACSL and VDAC that are responsible for channeling activated fatty acids through the MOM into the mitochondrial intermembrane space.

To examine the state of CPT1a in the MOM, we used an approach that combined sizing by mass and isolation using immunological methods. BNE of rat liver MOM extracts revealed the presence of several higher molecular mass bands that contained CPT1a, ACSL, and VDAC. Furthermore, immunoprecipitation with CPT1a-specific antibodies and antisera against ACSL and VDAC revealed a strong interaction between the proteins. These data strongly suggest that CPT1a forms hetero-oligomeric complexes with ACSL and VDAC and is part of an outer membrane fatty acid transfer complex.

EXPERIMENTAL PROCEDURES

Animals—Male Sprague-Dawley rats (200–400 g; Charles River, Wilmington, MA) had free access to food and water. All procedures were approved by the Case Western Reserve University Institutional Animal Care and Use Committee and performed in accordance with National Institutes of Health guidelines for care and use of animals in research.

Chemicals—Lubrol PX was obtained from ICI (London, United Kingdom). Chemically modified porcine trypsin was purchased from Promega. Protease inhibitor and protein phosphatase inhibitor mini tablets were from Roche Applied Science. Stock solutions were prepared by dissolving one tablet in 1 ml of Milli-Q water. Secondary antibodies and colorimetric reagents were purchased from Bio-Rad, and ECL reagents were from GE Healthcare. All other chemicals were from Sigma and were the highest available purity.

Antibodies—All antisera were raised in rabbits. Anti-CPT1a, anti-ACSL, and anti-VDAC1 antisera were prepared previously and stored at −60 °C. The CPT1a epitopes selected for immunization correspond to sequences ^{3}EAHQAVAFQFTVTPDG^{18}, ^{85}AKISRTLDTTGRMSSQTK^{102}, ^{230}NYVSDWWEEYIYLRGR^{245}, ^{617}QAMMDPKSTAEQRLK^{631}, and ^{731}FIHFHISSKFSSPETDSHRFGK^{752} (14). Anti-ACSL antiserum was prepared against the catalytically active full-length protein isolated from rat liver microsomes (15), and antiserum specific for VDAC1 was generated against a peptide corresponding to sequence ^{107}GKKNAKIKTGYKREH^{121} (16). The CPT1a-specific antibodies were isolated by affinity chromatography by coupling the peptides to SulfoLink resin (Pierce). For experiments using whole antisera, the antisera were precleared by centrifugation in an Airfuge (10 min, 160,000 × *g*).

Preparation of Rat Liver Mitochondria and MOMs—Rat liver mitochondria were isolated by differential centrifugation in 220 mM mannitol, 70 mM sucrose, and 5 mM MOPS (pH 7.4) (containing one mini tablet of protein phosphatase inhibitor/100 ml) and purified by Percoll gradient centrifugation (17). The outer membrane was isolated in high purity by the swell/shrink technique and discontinuous sucrose gradient centrifugation as described previously in detail (15). The isolated outer membranes were resuspended in 300 μl of 20 mM MOPS (pH 7.4) supplemented with 30 μl of protein phosphatase inhibitor stock solution and stored at −60 °C until analysis. For the BNE experiments, the isolated MOM was sonicated to eliminate contaminating and loosely membrane-associated proteins and re-isolated by discontinuous sucrose gradient centrifugation as described above.

BNE—BNE was performed as described (18) and is briefly summarized below. The sonicated MOM (300 μg of protein) was diluted with 150 μl of BNE buffer (50 mM imidazole (pH 7.0), 500 mM 6-aminocaproic acid, and 1 mM EDTA) and collected by centrifugation (Beckman Airfuge; 10 min, 160,000 × *g*) to remove MOPS. The pellet was resuspended in BNE buffer supplemented with Triton X-100 at a detergent/protein ratio of 3, kept on ice for 30 min with intermittent mixing with a micropipette, and then centrifuged using the Airfuge as described above. Coomassie Blue G-250 was added to the supernatant at a dye/detergent ratio of 8. The solubilized protein complexes were separated on a 3–12% gradient gel and subjected either to Western blotting or, after reduction, alkylation, and in-gel trypsin digestion, to LC-MS/MS analysis.

Solubilization of MOM—One mg of MOM in 20 mM MOPS was thawed and centrifuged in the Airfuge as described above. The resultant pellet was solubilized in 200 μl of immunoprecipitation buffer (4 mg of Lubrol PX, 500 mM NaCl, 25 mM sodium phosphate (pH 7.0), and 20 μl each of protease inhibitor and protein phosphatase inhibitor stock solutions). The mixture was placed on ice for 30 min with gentle mixing by magnetic stirrer and centrifuged in the Airfuge as described above. The resultant supernatant was used in immunoisolation experiments.

Immunoisolation of CPT1a—Two different approaches were used. In one method, protein G-conjugated beads saturated with affinity-purified anti-CPT1a antibodies directed against amino acids 230–245 were used to isolate CPT1a. In the second method, a mixture of all five affinity-purified anti-CPT1a antibodies was directly conjugated to CarboLink resin (Pierce) following the manufacturer's instruction. The supernatant from the solubilized MOM was added to 10 μg of protein G-bound IgG or CarboLink-conjugated IgG (equivalent to 10 μg of IgG), and the reaction was carried out overnight at 4 °C by end-over-end rotation. The resins were washed three times with a total of 900 μl of wash buffer (10 mM sodium phosphate (pH 7.0), 150 mM NaCl, and 1 mM EDTA) containing 0.5% Lubrol PX, followed by three additional washes lacking Lubrol PX. The immunoisolated proteins were eluted with 100 μl of 100 mM glycine HCl (pH 2.8) into 20 μl of 1.0 M Tris (pH 8.0) to neutralize to pH 7.0. Each eluted fraction was analyzed by SDS-PAGE and immunoblotting.

Immunoprecipitation with Anti-CPT1a, Anti-ACSL, and Anti-VDAC1 Antisera—The solubilized MOM extract (300 μg each) was incubated with precleared anti-CPT1a, anti-ACSL, or anti-VDAC1 antiserum (20 μl each), and each individual tube was incubated overnight at 4 °C by end-over-end rotation. The immunoprecipitated proteins were collected by centrifugation in the Airfuge as described above, and the tube and pellet were rinsed twice with 200 μl of Milli-Q water, resuspended in

Laemmli sample buffer, and subjected to SDS-PAGE (10% separating gel) and immunoblotting.

Western Blotting—Proteins separated by BNE and SDS-PAGE were transferred to PVDF membranes, and the membranes were probed with affinity-purified anti-CPT1a peptide antibody (^{230}NYVSDWWEEYIYLRGR^{245}), anti-ACSL polyclonal antiserum, or anti-VDAC1 peptide antiserum. The proteins were visualized colorimetrically or by enhanced chemiluminescent detection (14).

MALDI-TOF MS—α-Cyano-4-hydroxycinnamic acid was dissolved in a 1:1 mixture of acetonitrile and water containing 0.1% TFA to make a saturated matrix solution. Analyte (0.5 μl) was mixed with 0.5 μl of matrix and loaded on a MALDIchip™ plate. Mass spectra were collected using a prOTOF2000 system (PerkinElmer Life Sciences) in positive ion mode at an accelerating voltage of 1.7 kV. The MALDI-TOF mass spectrometer was calibrated immediately before the analysis using angiotensin II and ACTH fragment 18–39 (human). The MS-Fit search engine was used to match mass spectra using the Swiss-Prot Protein Database.

LC-MS/MS—Electrospray spectra were acquired on a Thermo Fisher LTQ Orbitrap mass spectrometer coupled to a nano-HPLC system (LC Packings). The flow rate was ~200 nl/min. Two μl of sample was injected onto the column. The mobile phases used were 0.1% formic acid in HPLC-grade water and 0.1% formic acid in HPLC-grade acetonitrile. Sample analyses were performed using data-dependent/dynamic exclusion with a repeat count of one to maximize coverage. The LTQ Orbitrap MS method employed eight full MS/MS scans following one full scan mass spectrum (400–2000 Da). All data files were searched against a rat subset taken from the Swiss-Prot Database using the Mascot database search engine (version 2.1.04, Matrix Science, London, United Kingdom). For these searches, the mass tolerance for the precursor and fragment ions was set to ±15 ppm and ±1 Da, respectively. Two missed cleavages were allowed for trypsin. Oxidized methionine and *S*-carbamidomethylation of cysteine were entered as differential modifications. The results of the searches were filtered by removing all peptide matches at an ion score of <25.

RESULTS

MOM Multiprotein Complexes Revealed by BNE—BNE was coupled with mass spectrometry to determine the oligomeric state of native CPT1a and proteins interacting with CPT1a. This method involves extraction with detergent and separation of the extracted protein complexes by nondenaturing electrophoresis. The method is gentle enough not to disrupt protein-protein interactions and is used routinely to study mitochondrial electron transport chain complexes and supercomplexes (19–21) and the subunit composition of the mitochondrial translocase of the outer membrane (22, 23).

For this experiment, the sonicated MOM was solubilized with Triton X-100, and the resultant supernatant was subjected to BNE. In preliminary experiments, the detergent/protein ratio was varied, and a ratio of 3 was found to be best to extract and resolve MOM protein complexes. As shown in Fig. 1, the MOM extract was resolved into five complexes with molecular masses ranging from 210 to 980 kDa (bands E to A). On Western blots, anti-CPT1a antibody (amino acids 230–245) decorated band A (980 kDa) and band D (280 kDa); anti-ACSL antiserum also recognized band A (980 kDa) and band D (280 kDa); and anti-VDAC1 antiserum cross-reacted with band A (980 kDa), band D (280 kDa), and band E (210 kDa). Under the experimental conditions, bands B and C (780 and 535 kDa) were not recognized by any of the three antibodies. A band at 128 kDa, but not monomeric CPT1a, was detected in the BNE gel by Western blotting.

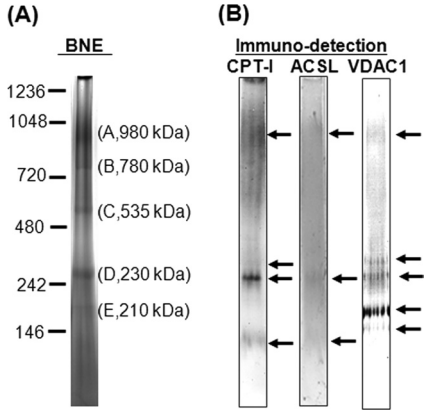

FIGURE 1. **Separation of MOM protein complexes by BNE.** The MOM was solubilized with Triton X-100 (Triton X-100/protein ratio of 3:1 (w/w)) at 4 °C and analyzed by BNE. *A*, five different protein complexes greater than 210 kDa but smaller than 980 kDa were separated by BNE. *B*, the separated complexes were analyzed by Western blotting using affinity-purified anti-CPT1a peptide (raised against amino acids 230–245), anti-ACSL, and anti-VDAC antisera.

The presence of these three proteins was further evaluated by mass spectrometry following in-gel digestion with trypsin of the respective bands. Analysis of the protein composition of each band by the more sensitive mass spectrometric method revealed that CPT1a was present in bands A (980 kDa), B (780 kDa), C (535 kDa), and D (280 kDa) but was absent from band E (210 kDa). Conversely, ACSL1 and VDAC1–3 were detected in all five bands. ACSL5 and ACSL6 were detected only in band E. Thus, bands containing CPT1a also contained different isoforms of ACSL and VDAC. Among the ACSL isoforms, ACSL1 dominated in terms of percent coverage, whereas ACSL5 and ACSL6 were represented by only a few specific peptides. Among the three VDAC isoforms, VDAC1 was the most abundant, but significant chain coverage was observed also with VDAC2 and VDAC3. The sequence coverage obtained by LC-MS/MS of the three proteins is given in Table 1, and the full list of identified proteins is provided in supplemental Table S1. These data suggest that CPT1a can associate to form homo- and/or hetero-oligomeric complexes containing metabolically relevant proteins, *i.e.* ACSL and VDAC isoforms.

Analysis of Immunoisolated CPT1a Protein Complexes—We used immunoisolation of CPT1a as an alternative approach to BNE to determine whether protein complexes with the same or similar composition can be isolated. In preliminary experiments, various detergents (Triton X-100, Triton X-114, dodecyl maltoside, Lubrol PX, digitonin, and Zwittergent 3–10, all 2% (w/v)) and buffer conditions were tested to solubilize CPT1a from the MOM. CPT1a was best extracted with 2% Lubrol PX, 500 mM NaCl, and 25 mM phosphate (pH 7.0). This buffer composition was used for all further experiments.

TABLE 1

LC-MS/MS analysis of protein complexes isolated by BNE

The sonicated MOM (300 μg) was extracted and subjected to BNE as described under "Experimental Procedures." Each band was excised, reduced, and alkylated, followed by in-gel digestion and analysis by LC-MS/MS.

BNE band/ protein name	Accession no.	Protein molecular mass	Coverage
		Da	*%*
A (980 kDa)			
CPT1a	P32198	88,069	29
ACSL1	P18163	78,128	57
VDAC1	Q9Z2L0	30,737	52
VDAC2	P81155	31,726	30
VDAC3	Q9R1Z0	30,778	15
B (780 kDa)			
CPT1a	P32198	88,069	20
ACSL1	P18163	78,128	59
VDAC1	Q9Z2L0	30,737	37
VDAC2	P81155	31,726	41
VDAC3	Q9R1Z0	30,778	26
C (535 kDa)			
CPT1a	P32198	88,069	23
ACSL1	P18163	78,128	60
VDAC1	Q9Z2L0	30,737	46
VDAC2	P81155	31,726	30
VDAC3	Q9R1Z0	30,778	30
D (230 kDa)			
CPT1a	P32198	88,069	1
ACSL1	P18163	78,128	60
VDAC1	Q9Z2L0	30,737	76
VDAC2	P81155	31,726	18
VDAC3	Q9R1Z0	30,778	14
E (210 kDa)			
ACSL1	P18163	78,128	60
ACSL5	O88813	76,405	5
ACSL6	P33124	78,180	2
VDAC1	Q9Z2L0	30,737	76
VDAC2	P81155	31,726	41
VDAC3	Q9R1Z0	30,778	22

Affinity-purified anti-CPT1a IgG (amino acids 230–245) was immobilized onto protein G beads and incubated with MOM extract in a Pierce spin column. After the column was drained and washed, bound proteins were eluted with 100 mM glycine (pH 2.8) directly into a predetermined volume of 1.0 M Tris (pH 8.0) to restore the pH to ~7.0 as described under "Experimental Procedures." The eluted fraction was subjected to SDS-PAGE and analyzed by protein staining (supplemental Fig. S1); by Western blotting (Fig. 2*A*); and after in-gel digestion, by MALDI-TOF MS analysis (supplemental Table S2). After the MOM was solubilized with 2% Lubrol PX, CPT1a, ACSL, and VDAC were in the supernatant and were not detectable in the pellet. The flow-through showed the same protein pattern as the supernatant but did not contain CPT1a (Fig. 2*A*, Western blot). Proteomic analysis of the eluted fraction following SDS-PAGE separation revealed the presence of not only CPT1a but also ACSL and VDAC (supplemental Fig. S1 and Table S2). Using anti-CPT1a IgG-coupled protein G beads for isolation of CPT1a resulted in the release of a large amount of IgG, which interfered with subsequent mass spectrometric analysis. The presence of IgG can mask or weaken the signal of other proteins of similar molecular mass retained by the antibodies. For example, very long chain acyl-CoA synthetase was detected in the IgG band (supplemental Fig. S1 and Table S2). To eliminate the interference by IgG and further enhance recognition and capture of CPT1a, a mixture of five affinity-purified anti-CPT1a antibodies was directly coupled to CarboLink and used in immunocapture experiments. As shown in Fig. 2*B* (*lower panel*), the use of covalent binding of the affinity-purified anti-CPT1a IgGs to the resin allowed elution of CPT1a without co-release of IgG, as seen with protein G. The additional advan-

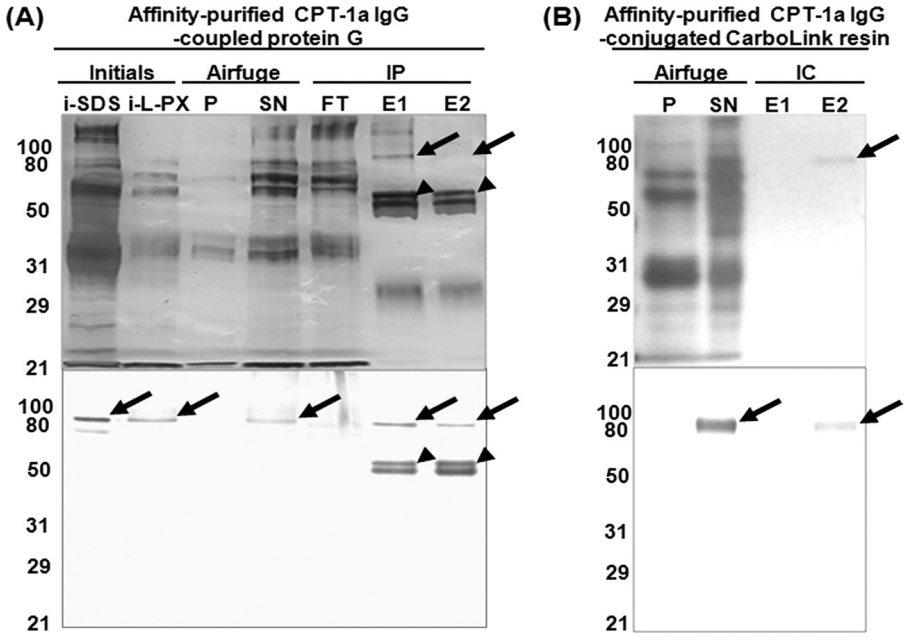

FIGURE 2. **Immunoisolation of CPT1a and proteins associated with CPT1a.** *A*, *upper panel*, SDS-PAGE separation and silver staining of proteins immunoprecipitated (*IP*) with affinity-purified anti-CPT1a antibodies coupled to protein G beads; *lower panel*, immunoblot analysis of the starting material (initial MOM solubilized with SDS sample buffer (*i-SDS*) and initial MOM solubilized with 2% Lubrol PX (*i-L-PX*)), the pellet after Lubrol PX extraction (Airfuge; *P*), and the Lubrol PX supernatant (Airfuge; *SN*) with affinity-purified anti-CPT1a antibodies. *Arrows* and *arrowheads* show CPT1a and anti-CPT1a antibodies, respectively. *B*, immunocapture (*IC*) of CPT1a and associated proteins with a mixture of five affinity-purified anti-CPT1a antibodies directly coupled to CarboLink. In the eluate, CPT1a, but not anti-CPT1a antibodies, was detected. *FT*, flow-through with either protein G or CarboLink; *E1* and *E2*, first and second eluents from either protein G- or CarboLink-coupled IgG, respectively.

tage of using five rather than one antibody is that our five individual antibodies are directed to different epitopes on CPT1a, thus increasing the chance of capturing the native enzyme. A further advantage in using IgG-coupled resin is that it can be used repeatedly. With silver staining, the eluent contained only one protein band at 88 kDa, which was decorated by anti-CPT1a antibody in immunoblots. The eluent from the resin-linked IgG system was further analyzed by in-solution digestion with trypsin, followed by LC-MS/MS. This proteomics approach identified CPT1a with 39% sequence coverage. ACSL1 was identified with 27% coverage, and ACSL6 was identified by one peptide specific for this isoform. VDAC1 also was identified with three peptides (Table 2). A full list of identified proteins is provided in supplemental Table S3.

Co-immunoprecipitation of CPT1a, ACSL, and VDAC—All three approaches described above, *i.e.* BNE and immunoprecipitation with anti-CPT1a antibodies coupled to protein G beads or coupled directly to CarboLink resin, suggested that CPT1a, ACSL, and VDAC1 are associated with one another. Antisera against all three proteins are available, and we tested whether anti-CPT1a antiserum can co-immunoprecipitate ACSL and VDAC1 and, conversely, whether antisera against ACSL and VDAC can co-immunoprecipitate CPT1a plus VDAC1 and CPT1a plus ACSL, respectively. Precleared antisera were used for co-immunoprecipitation as described under Experimental Procedures" and in the experimental protocol outlined in the legend to Fig. 3*A*. The results of these co-immunoprecipitations are shown in Fig. 3*B*. Anti-CPT1a antiserum precipitated CPT1a antigen as well as ACSL and VDAC proteins (*upper panel*); co-immunoprecipitation with anti-VDAC1 antiserum (*middle panel*) immunoprecipitated not only VDAC antigen but also CPT1a and ACSL; and anti-ACSL antiserum (*lower panel*) pulled down ACSL along with VDAC and CPT1a. These co-immunoprecipitation results confirmed that CPT1a, ACSL, and VDAC proteins are physically associated with one another.

TABLE 2

Identification of proteins immunocaptured with CarboLink resin-coupled affinity-purified anti-CPT1a antibody

CPT1a and associated proteins were immunocaptured with a mixture of five affinity-purified anti-CPT1a antibodies directly conjugated to CarboLink resin as described under "Experimental Procedures." Immunocaptured proteins were reduced and alkylated and then digested with trypsin for LC-MS/MS analysis.

Protein	Score	Molecular mass	Coverage	Accession no.	No. of unique peptides (hits)
		Da	*%*		
ACSL1	779	78,128	16	P18163	10
CPT1a	1605	88,069	34	P32198	30
VDAC1	248	30,737	19	Q9Z2L0	3

DISCUSSION

Using a multifaceted approach, *i.e.* BNE and immunoprecipitation/immunocapture, we have demonstrated a strong physical interaction between the MOM proteins CPT1a, ACSL, and VDAC. Such interactions are expected if CPT1a, ACSL, and VDAC form a complex in the MOM, and the complex withstands detergent extraction from the membrane and isolation by BNE and immunocapture. All three proteins are highly hydrophobic integral membrane proteins with two (CPT1a and ACSL) or more (VDAC) transmembrane segments. Because the complex resists the high ionic strength encountered during immunoisolation, hydrophobic interactions between the individual proteins must form and stabilize the complex. The presence of CPT1a, ACSL, and VDAC in several bands with differing molecular masses suggests the presence of hetero-oligomeric complexes with differing stoichiometry of the individual components. Other proteins were identified by mass

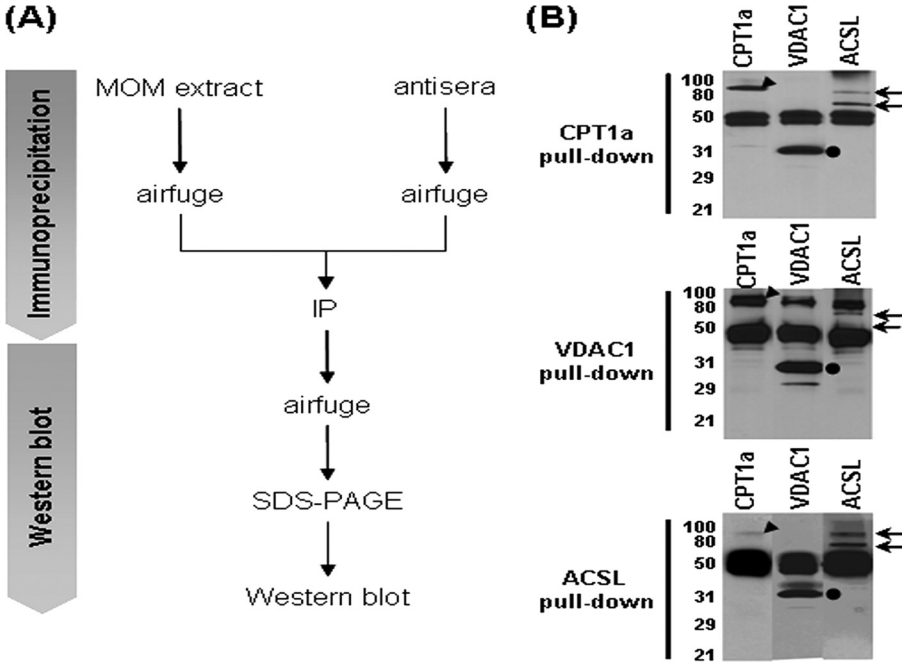

FIGURE 3. **Co-immunoprecipitation using anti-CPT1a, anti-ACSL, and anti-VDAC1 antisera.** Anti-CPT1a, anti-ACSL, or anti-VDAC antiserum was precleared by centrifugation (Airfuge, 10 min, 160,000 × *g*), and 20-μl aliquots each were mixed with Lubrol PX supernatant from the MOM (300 μg). The immunoprecipitate (*IP*; Airfuge, 10 min, 30 p.s.i.) was subjected to SDS-PAGE (*A*) and Western blot analysis (*B*). *B*, *upper*, *middle*, and *lower panels*, immunoprecipitation with anti-CPT1a, anti-VDAC1, and anti-ACSL antisera, respectively. *Arrowheads*, CPT1a; *closed circles*, VDAC1; *arrows*, ACSL.

spectrometry, and because the Mascot scores were higher than the acceptance criteria as described under "Experimental Procedures," we elected to list these proteins without discussing the data. The list of these other proteins, identified in each BNE band, is provided in supplemental Table S1.

Using chemical cross-linking of rat liver mitochondria and yeast mitochondria expressing CPT1a followed by SDS-PAGE, Faye *et al.* (12) reported that CPT1a exists as a homo-oligomeric trimer. Upon BNE and size exclusion chromatography of rat liver mitochondrial extracts, CPT1a behaved as a hexamer. In these experiments, CPT1a was identified by Western blotting, and the assignment of the observed higher molecular mass species as oligomeric forms of CPT1a was based on the finding that these higher molecular masses could be accounted for by multiples of the monomeric mass of CPT1a. In subsequent studies, Jenei *et al.* (13) reported that CPT1a exists as a hexamer and that the oligomerization state is reduced to trimers during isolation and storage of the mitochondria. The presence of other proteins was not investigated in the respective bands or fractions in either of these two studies.

The data from immunocapture, reverse immunoprecipitation of CPT1a with anti-ACSL and anti-VDAC1 antisera, and BNE experiments indicate that these three proteins associate in the MOM to form hetero-oligomeric complexes of different molecular masses. This raises a question about the function(s) of these complexes as well as questions about membrane topology and the stoichiometry of the individual component proteins.

The migration of protein complexes on BNE depends on the amount of the negatively charged dye bound by the complexes. The size estimation of complexes is not accurate because dye-binding sites can be masked by protein-protein interactions between the individual proteins present in the complexes. Furthermore, the surface charge of the complex is affected by the hydrophilic or hydrophobic nature of the individual proteins that make up the complexes, especially with membrane proteins where lipids also may be present. The dimeric form of ACSL has been reported as the active form in rat and in *S. cerevisiae* (24, 25), and VDAC has been described as a dimer or tetramer (26, 27). On the basis of these findings, we estimated the possible composition of the band at 280 kDa as consisting of a CPT1a monomer, an ACSL dimer, and a VDAC dimer that yield a sum of 296 kDa. The other bands require direct determination of the stoichiometry.

Previously, we showed that in rat liver mitochondria, PA22 inhibits oxidation of palmitate and palmitoyl-CoA but does not inhibit palmitoylcarnitine oxidation or CPT1a activity (3). The conundrum of PA22 inhibition of palmitoyl-CoA oxidation without affecting palmitoylcarnitine oxidation suggested to us that there was a step in palmitoyl-CoA oxidation that occurred before CPT1a but after ACSL that had not been identified. We then focused on the step for moving palmitoyl-CoA from its site of production, the outer surface of outer membrane, to CPT1a. We entertained VDAC as a candidate to explain the inhibition of palmitoyl-CoA oxidation without inhibition of palmitoylcarnitine oxidation. The data from these published studies showed that PA22 interacts with VDAC. Therefore, VDAC appears to be an appropriate target that moves anions into the intermembrane space. If that step is inhibited, the active site of CPT1a must face in, not out.

On the basis of these data, we postulated a model in which long chain fatty acids are activated by ACSL on the cytosolic side of the MOM and the activated acyl-CoA esters gain access to the mitochondrial intermembrane space via VDAC. The acyl-CoAs are then converted to acylcarnitine by CPT1a on the intermembrane side of the MOM (28). In this model, the catalytic site of ACSL faces the cytosol, and the catalytic site of CPT1a faces the intermembrane space, in agreement with the data from Murthy and Pande (29). However, the approach of Zammit and co-workers (30), using agarose-coupled acyl-CoA in which the acyl-CoA was rendered incapable of crossing the MOM, suggested the opposite orientation for the catalytic site of CPT1a. Thus, there is evidence to support both the cytosolic and the intermembrane orientation of the catalytic site of CPT1a. Structural studies of the topology of CPT1a in the outer membrane are required to resolve this issue.

Our data show that CPT1a was immunocaptured with ACSL and VDAC, consistent with the postulation that they compose an outer membrane fatty acid transfer complex (28). The catalytic advantage of physical association or interaction between ACSL, VDAC, and CPT1a is that it favors direct channeling of the intermediates from the outer surface of the MOM into the intermembrane space. A model that depicts the coordinated action of ACSL, VDAC, and CPT1a in channeling activated fatty acids through the MOM is presented in Fig. 4. In this model, long chain fatty acids are activated by ACSL on the cytosolic side of the MOM, and the activated fatty acids move into the intermembrane space through VDAC, where the acyl-CoAs are converted to the respective acylcarnitines by CPT1a.

In an alternative topological model of CPT1a, the catalytic (and regulatory) site faces the cytosol (30, 31), and the homo-oligomerization of CPT1a monomers to trimers or hexamers provides the structural basis for a channel allowing the acylcarnitine formed on the cytosolic side of the MOM to enter the intermembrane space (12, 13). Except for the formation of a channel for acylcarnitine translocation, it is difficult to envisage from the available experimental data the functional advantage of CPT1a homo-oligomerization. Based on target size analysis, the functional or catalytic unit of CPT1a is the monomeric form (32). Thus, in the homo-oligomeric state, each monomer functions independently, with no cooperation between the individual monomers. Furthermore, the homo-oligomerization state of CPT1a is not altered by fasting or by streptozotocin-induced diabetes (12), conditions known to result in increased catalytic activity and decreased malonyl-CoA sensitivity. Thus, neither the catalytic activity nor the regulatory property of CPT1a is affected by homo-oligomerization.

In addition to the above studies showing hetero- and homo-oligomerization of CPT1a, there also are reports on the association of CPT1b with the fatty acid transport proteins CD36/fatty acid translocase and FATP1 (33–35) in heart and skeletal muscle mitochondria. This association of CPT1b with CD36 or FATP1 is reported to facilitate the mitochondrial oxidation of long chain fatty acids. We documented the presence of CD36/fatty acid translocase in highly purified rat liver MOMs (16); however, in the present study using mass spectrometry, we

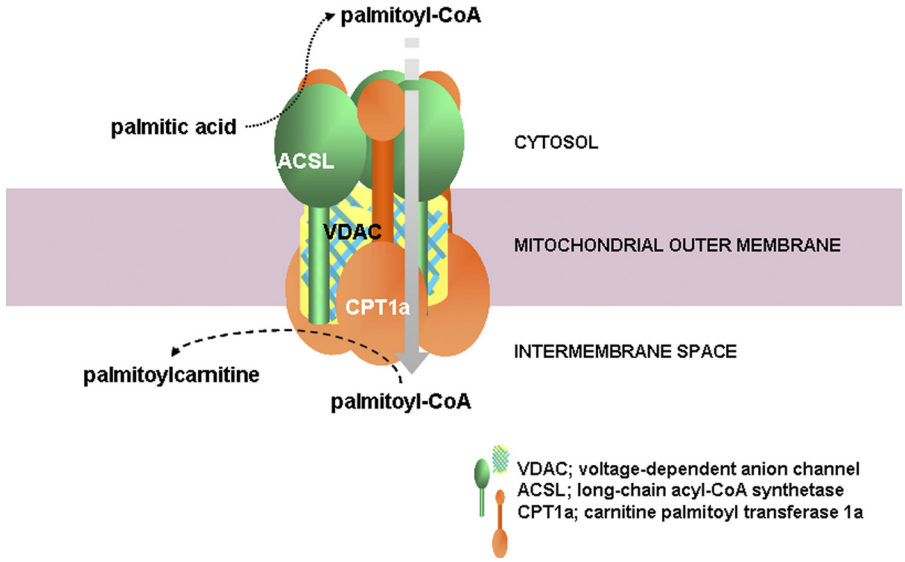

FIGURE 4. **Proposed model of the hetero-oligomeric MOM complex consisting of CPT1a, ACSL, and VDAC.** Palmitoyl-CoA formed by ACSL in the cytosol is channeled into the intermembrane space through VDAC, where it is transesterified to palmitoylcarnitine by CPT1a.

could not detect CD36 in either BNE or immunoisolation experiments. Also, the oxidation of palmitoyl-CoA and palmitoylcarnitine in heart and skeletal muscle mitochondria isolated from CD36 knock-out mice was identical to that in wild-type mice (36).

In addition to CPT1 and ACSL, VDAC has been shown to associate with other proteins, forming heteromeric complexes involved in mitochondrial energy exchange and in cholesterol transport into the mitochondrial matrix for steroid synthesis (37–39). In mitochondrial contact sites, VDAC can be associated with the adenine nucleotide translocator, an integral inner membrane protein, and with hexokinase in the cytosol or creatine kinase in the mitochondrial intermembrane space. These complexes play an important role in mitochondrial energy exchange as well as in apoptosis (37, 39). VDAC forms a hetero-oligomeric complex with the adenine nucleotide translocator and the 18-kDa benzodiazepine-binding protein, called the peripheral benzodiazepine receptor. In steroidogenic tissues, the receptor complex represents the rate-limiting step in steroidogenesis through regulation of cholesterol transport from the cytoplasm to the mitochondrial matrix (38).

The common denominator in the heteromeric complexes described above is the MOM protein VDAC. The question then arises as to how VDAC can perform different transport functions and what governs its association with proteins of the mitochondrial outer and inner membranes, cytosol, and mitochondrial intermembrane space. The answer possibly lies in the fact that 1) VDAC is the most abundant protein in the MOM, representing ~5–10% of the total MOM protein; 2) VDAC is expressed in three isoforms (VDAC1–3), and all three isoforms are present in most tissues but in different amounts (40); and 3) all three VDAC isoforms are post-translationally modified mainly by phosphorylation and acetylation (41–44).

In conclusion, CPT1a, which catalyzes the first committed and regulated step in mitochondrial fatty acid oxidation, forms hetero-oligomeric complexes of different molecular masses with ACSL and VDAC in the MOM. The functional relevance of these different complexes is unknown at present. Further studies are needed to determine the stoichiometry of individual protein components as well as their functional relevance to these complexes in different nutritional and disease states such as feeding, starvation, and diabetes.

Acknowledgments—We thank Dr. Anne Distler for showing that sonication removes contaminating proteins from MOM and Michelle Jennings for the initial BNE experiments during a research rotation. We also thank Drs. Bernard Tandler and Tomas Radivoyevitch and the Writing with Style group of the Hoppel laboratory for editorial assistance.

REFERENCES

1. Bhuiyan, J., Pritchard, P. H., Pande, S. V., and Seccombe, D. W. (1995) *Metabolism* **44,** 1185–1189
2. Pusnik, M., Charrière, F., Mäser, P., Waller, R. F., Dagley, M. J., Lithgow, T., and Schneider, A. (2009) *Mol. Biol. Evol.* **26,** 671–680
3. Turkaly, P., Kerner, J., and Hoppel, C. (1999) *FEBS Lett.* **460,** 241–245
4. Felgner, P. L., Messer, J. L., and Wilson, J. E. (1979) *J. Biol. Chem.* **254,** 4946–4949
5. König, T., Stipani, I., Horvàth, I., and Palmieri, F. (1982) *J. Bioenerg. Biomembr.* **14,** 297–305
6. Colombini, M., Yeung, C. L., Tung, J., and König, T. (1987) *Biochim. Biophys. Acta* **905,** 279–286
7. Cesar Mde, C., and Wilson, J. E. (2004) *Arch. Biochem. Biophys.* **422,** 191–196
8. Anflous, K., Armstrong, D. D., and Craigen, W. J. (2001) *J. Biol. Chem.* **276,** 1954–1960
9. Anflous-Pharayra, K., Lee, N., Armstrong, D. L., and Craigen, W. J. (2011) *Biochim. Biophys. Acta* **1807,** 150–156
10. Craigen, W. J., and Graham, B. H. (2008) *J. Bioenerg. Biomembr.* **40,** 207–212
11. McGarry, J. D., and Brown, N. F. (1997) *Eur. J. Biochem.* **244,** 1–14
12. Faye, A., Esnous, C., Price, N. T., Onfray, M. A., Girard, J., and Prip-Buus, C. (2007) *J. Biol. Chem.* **282,** 26908–26916
13. Jenei, Z. A., Borthwick, K., Zammit, V. A., and Dixon, A. M. (2009) *J. Biol. Chem.* **284,** 6988–6997
14. Hoppel, C., Kerner, J., Turkaly, P., Minkler, P., and Tandler, B. (2002) *Anal. Biochem.* **302,** 60–69

15. Hoppel, C., Kerner, J., Turkaly, P., and Tandler, B. (2001) *Arch. Biochem. Biophys.* **392,** 321–325
16. Distler, A. M., Kerner, J., Peterman, S. M., and Hoppel, C. L. (2006) *Anal. Biochem.* **356,** 18–29
17. Hoppel, C. L., Kerner, J., Turkaly, P., Turkaly, J., and Tandler, B. (1998) *J. Biol. Chem.* **273,** 23495–23503
18. Wittig, I., Braun, H. P., and Schägger, H. (2006) *Nat. Protoc.* **1,** 418–428
19. Rosca, M. G., Vazquez, E. J., Kerner, J., Parland, W., Chandler, M. P., Stanley, W., Sabbah, H. N., and Hoppel, C. L. (2008) *Cardiovasc. Res.* **80,** 30–39
20. Schägger, H. (1995) *Methods Enzymol.* **260,** 190–202
21. Schägger, H. (2001) *Methods Cell Biol.* **65,** 231–244
22. Nakamura, Y., Suzuki, H., Sakaguchi, M., and Mihara, K. (2004) *J. Biol. Chem.* **279,** 21223–21232
23. Werhahn, W., Niemeyer, A., Jänsch, L., Kruft, V., Schmitz, U. K., and Braun, H. (2001) *Plant Physiol.* **125,** 943–954
24. Bar-Tana, J., Rose, G., and Shapiro, B. (1973) *Biochem. J.* **135,** 411–416
25. Li, H., Melton, E. M., Quackenbush, S., DiRusso, C. C., and Black, P. N. (2007) *Biochim. Biophys. Acta* **1771,** 1246–1253
26. Keinan, N., Tyomkin, D., and Shoshan-Barmatz, V. (2010) *Mol. Cell. Biol.* **30,** 5698–5709
27. Zalk, R., Israelson, A., Garty, E. S., Azoulay-Zohar, H., and Shoshan-Barmatz, V. (2005) *Biochem. J.* **386,** 73–83
28. Kerner, J., and Hoppel, C. (2000) *Biochim. Biophys. Acta* **1486,** 1–17
29. Murthy, M. S., and Pande, S. V. (1987) *Proc. Natl. Acad. Sci. U.S.A.* **84,** 378–382
30. Fraser, F., Corstorphine, C. G., and Zammit, V. A. (1997) *Biochem. J.* **323,** 711–718
31. Zammit, V. A., Fraser, F., and Orstorphine, C. G. (1997) *Adv. Enzyme Regul.* **37,** 295–317
32. Zammit, V. A., Corstorphine, C. G., and Kolodziej, M. P. (1989) *Biochem. J.* **263,** 89–95
33. Campbell, S. E., Tandon, N. N., Woldegiorgis, G., Luiken, J. J., Glatz, J. F., and Bonen, A. (2004) *J. Biol. Chem.* **279,** 36235–36241
34. Schenk, S., and Horowitz, J. F. (2006) *Am. J. Physiol. Endocrinol. Metab.* **291,** E254–E260
35. Sebastián, D., Guitart, M., García-Martínez, C., Mauvezin, C., Orellana-Gavaldà, J. M., Serra, D., Gómez-Foix, A. M., Hegardt, F. G., and Asins, G. (2009) *J. Lipid Res.* **50,** 1789–1799
36. King, K. L., Stanley, W. C., Rosca, M., Kerner, J., Hoppel, C. L., and Febbraio, M. (2007) *Arch. Biochem. Biophys.* **467,** 234–238
37. Brdiczka, D. G., Zorov, D. B., and Sheu, S. S. (2006) *Biochim. Biophys. Acta* **1762,** 148–163
38. Gavish, M., Bachman, I., Shoukrun, R., Katz, Y., Veenman, L., Weisinger, G., and Weizman, A. (1999) *Pharmacol. Rev.* **51,** 629–650
39. Vyssokikh, M., and Brdiczka, D. (2004) *Mol. Cell. Biochem.* **256–257,** 117–126
40. Sampson, M. J., Lovell, R. S., and Craigen, W. J. (1997) *J. Biol. Chem.* **272,** 18966–18973
41. Deng, W. J., Nie, S., Dai, J., Wu, J. R., and Zeng, R. (2010) *Mol. Cell. Proteomics* **9,** 100–116
42. Distler, A. M., Kerner, J., and Hoppel, C. L. (2007) *Biochim. Biophys. Acta* **1774,** 628–636
43. Kim, S. C., Sprung, R., Chen, Y., Xu, Y., Ball, H., Pei, J., Cheng, T., Kho, Y., Xiao, H., Xiao, L., Grishin, N. V., White, M., Yang, X. J., and Zhao, Y. (2006) *Mol. Cell* **23,** 607–618
44. Schwer, B., Eckersdorff, M., Li, Y., Silva, J. C., Fermin, D., Kurtev, M. V., Giallourakis, C., Comb, M. J., Alt, F. W., and Lombard, D. B. (2009) *Aging Cell* **8,** 604–606